

Sensitivity analysis and parameter identifiability for colloid transport in geochemically heterogeneous porous media

Ning Sun,¹ Ne-Zheng Sun,² Menachem Elimelech,¹ and Joseph N. Ryan³

Abstract. Effective use of colloid transport models for heterogeneous subsurface porous media requires the development of methodologies to identify the key model parameters. The inverse problem of a two-dimensional model for colloid transport in geochemically heterogeneous porous media is systematically investigated in this paper. Sensitivity analysis prior to the parameter identification provided valuable insights into the identifiability of the six model parameters. The hydraulic conductivity and longitudinal dispersivity were identified from tracer breakthrough data and then were used in the remaining parameter identification. The four colloid deposition and release parameters, favorable (fast) colloid deposition rate coefficient, geochemical heterogeneity, unfavorable (slow) colloid deposition rate coefficient, and colloid release rate coefficient from the unfavorable surface fraction, were found to be highly interrelated, and the inverse solution of the four-parameter set was not unique. When either the geochemical heterogeneity or favorable colloid deposition rate coefficient is known, the other three colloid deposition and release parameters can be identified via the inverse solution if the duration of the colloid injection is sufficiently long. The colloid release rate coefficient, however, cannot be identified when using a short (pulse-like) colloid injection. Neglecting the colloid release rate results in estimation errors of the other model parameters and thus adversely affects the subsequent prediction of colloid transport.

1. Introduction

There is a growing interest in modeling the transport of colloidal particles in subsurface porous media. To date, practical use of colloid transport models has been limited to one-dimensional transport in homogeneous porous media. Most models attempt to fit experimental data of colloid, bacteria, or virus transport in packed columns. Extension of colloid transport modeling from laboratory scale to the field scale is a rather challenging step.

To effectively apply colloid transport models, the model parameters must be known. However, most model parameters representing the properties of heterogeneous subsurface porous media or colloidal particles are usually unknown and need to be properly identified. Hence it is imperative that the inverse problem of colloid transport in heterogeneous subsurface porous media be solved.

There has been extensive research on the inverse problem in studies of groundwater flow and solute transport in the past several decades. Comprehensive reviews are given by Yeh [1986], Kuiper [1986], Carrera [1998], Ginn and Cushman [1990], Sun [1994], and McLaughlin and Townley [1996]. Most published studies were concerned with the identification of hydraulic conductivity and storage coefficient based on head observations. Only a limited number of studies, however, dealt

with the identification of dispersion parameters and contaminant sources based on solute concentration observations [e.g., Mishra and Parker, 1989; Sun and Yeh, 1990; Harvey and Gorelick, 1995].

In studies of colloid transport, additional model parameters (other than hydraulic and colloid dispersion parameters), namely, colloid deposition and release parameters, need to be identified. Fundamental theories of colloid deposition/filtration [Tien, 1989; Elimelech *et al.*, 1995] and colloid release [Ruckenstein and Prieve, 1976] can provide analytical expressions for particle deposition or release rate coefficients (constants) in ideal model systems. Several investigations used such expressions for colloid deposition or release rate constants in colloid transport models [e.g., Johnson *et al.*, 1996]. However, in real subsurface systems the assumptions under which these expressions for colloid deposition and release were derived are not usually satisfied. Alternatively, several studies adopted a relatively simple colloid transport model and derived analytical solutions [e.g., Yan, 1996; Sim and Chrysikopoulos, 1995]. The model parameters were then determined by either solving the inverse function of the analytical solution [Yan, 1996] or carrying out controlled column experiments [Ryan and Gschwend, 1994; Harmand *et al.*, 1996]. These relatively simple models, however, cannot properly describe colloid transport in natural subsurface porous media, which are inherently heterogeneous.

To analyze field experimental data, Harvey and Garabedian [1991] applied the moment analysis result of Valocchi [1985] to estimate the collision (attachment) efficiency of bacteria in groundwater. This method has also been used by Pieper *et al.* [1997] and Ryan *et al.* [1999] to determine the collision efficiency of viruses and colloids in a sandy aquifer. Since colloid breakthrough curves are usually highly skewed, this may lead to difficulties in applying the moment analysis. Only a few studies have identified the parameters of colloid transport

¹Environmental Engineering Program, Department of Chemical Engineering, Yale University, New Haven, Connecticut.

²Department of Civil and Environmental Engineering, University of California, Los Angeles, California.

³Department of Civil, Environmental, and Architectural Engineering, University of Colorado, Boulder, Colorado.

Copyright 2001 by the American Geophysical Union.

Paper number 2000WR900291.
0043-1397/01/2000WR900291\$09.00

models numerically. Nonlinear least squares curve fitting was used to identify the parameters of relatively simple colloid transport models, such as one-dimensional kinetics models or one-dimensional pseudokinetics colloid transport models [Bales *et al.*, 1991; Sainers *et al.*, 1994a, 1994b; Roy and Dzombak, 1996; Penrod *et al.*, 1996]. For more complicated models, such as two-dimensional models or second-order kinetics models, model parameters were estimated only by manual curve fitting [McCaulou *et al.*, 1994; Sainers *et al.*, 1994a, 1994b; Roy and Dzombak, 1996; Sim and Chrysikopoulos, 1998].

The solution of inverse problems involves much more than simple curve fitting. It is essential to know the conditions under which the unknown parameters are identifiable, whether the observation data are sufficient for inverse solution, how sensitive is the inverse solution to observation errors, and what is the best experimental design for identifying a specified parameter. In this paper, we present a two-dimensional coupled flow and colloid transport model to study the identifiability of six colloid transport related parameters: (1) hydraulic conductivity, (2) longitudinal dispersivity, (3) geochemical heterogeneity, (4) favorable (fast) particle deposition rate coefficient, (5) unfavorable (slow) particle deposition rate coefficient, and (6) particle release rate coefficient from the unfavorable (for deposition) surface fraction. In this procedure it is assumed that the flow field is in steady state and that the transport of colloids does not affect the flow field. As a result, the flow equation and colloid transport equation can be solved sequentially, and the six hydraulic and colloid transport parameters are identified step by step. The weighted least squares criterion is chosen to define the performance function, and the formulated optimization problem is solved by the Gauss-Newton-Levenberg-Marquardt method.

2. The Forward Problem for Colloid Transport

A two-dimensional model capable of simulating colloid transport in geochemically heterogeneous porous media will be presented prior to the inverse problem formulation and analysis. The model consists of three coupled equations, a flow equation, a colloid transport equation, and a colloid deposition and release equation, as described in sections 2.1–2.4.

2.1. Flow Field

The transient flow equation is generally described by [e.g., Bear, 1972]

$$S_s \frac{\partial h}{\partial t} = \nabla \cdot (\mathbf{K} \nabla h), \quad (1)$$

where h is the hydraulic head, t is the time, S_s is the specific storage coefficient, and \mathbf{K} is the hydraulic conductivity. Under natural gradient flow conditions the fluid is usually in steady state flow. Hence the spatially distributed hydraulic heads are determined for a steady state flow field and then used to calculate the fluid velocity by applying Darcy's law

$$\mathbf{q} = -\mathbf{K} \nabla h, \quad (2)$$

where ∇h is the hydraulic head gradient and \mathbf{q} is Darcy's velocity. The average pore velocity (V), which usually appears in the transport equation, is the ratio of Darcy's velocity to porosity.

2.2. Colloid Transport Equation

The colloid transport equation can be derived from mass balance of colloids over a representative elementary volume

(REV) of a porous medium. There are three main mechanisms controlling colloid transport: hydrodynamic dispersion, advection, and colloid transfer between the stationary solid matrix and the mobile colloidal phase through colloid deposition and release. These mechanisms can be described by the generalized advection-dispersion equation in terms of the colloid number concentration n [Johnson *et al.*, 1996],

$$\frac{\partial n}{\partial t} = \nabla \cdot (\mathbf{D} \nabla n) - \nabla \cdot (\mathbf{V} n) - \frac{f}{\pi a_p^2} \frac{\partial \theta}{\partial t}, \quad (3)$$

where \mathbf{V} is the interstitial velocity, θ is the fractional surface coverage of deposited colloids, f is the specific surface area, a_p is the colloid radius, and \mathbf{D} is the hydrodynamic dispersion coefficient. For the two-dimensional transport problem considered here, the components of the hydrodynamic dispersion coefficient are related to the particle Stokes-Einstein diffusivity D_d and the components of the interstitial velocity (\bar{V}_i and \bar{V}_j) by

$$D_{ij} = \alpha_T \bar{V} \delta_{ij} + (\alpha_L - \alpha_T) \frac{\bar{V}_i \bar{V}_j}{\bar{V}} + D_d T \delta_{ij}, \quad (4)$$

where α_L and α_T are the longitudinal and transverse dispersivities, respectively, T is the porous medium tortuosity, δ_{ij} is the Kronecker delta, and \bar{V} is the geometric average of \bar{V}_i and \bar{V}_j . Note that a unidirectional flow along the x direction is assumed with $\bar{V}_j = 0$ in the simulations presented in this paper.

2.3. Patchwise Geochemical Heterogeneity of Porous Media

Ferric oxyhydroxide coatings are the main source of geochemical heterogeneity of the solid matrix in many surficial aquifers containing iron-bearing minerals [e.g., Scholl *et al.*, 1990; Scholl and Harvey, 1992; Coston *et al.*, 1995; Ryan *et al.*, 1999]. These coatings on mineral grain surfaces provide favorable sites (area) for colloid deposition because they are positively charged, whereas the majority of subsurface colloidal particles are negatively charged. Here we adopt the patch model [Song *et al.*, 1994] to describe the geochemical heterogeneity of subsurface porous media. The model is characterized by the geochemical heterogeneity parameter λ , which is defined as the ratio of the surface area favorable for deposition (i.e., particle deposition onto this area is not hindered by colloidal interactions and is transport-limited) to the total interstitial surface area over a representative elementary volume of a porous medium. Note that colloid deposition onto the unfavorable surface fraction ($1 - \lambda$) is hindered by electrostatic double layer repulsion because particles and unfavorable surface fraction are both negatively charged.

2.4. Colloid Deposition and Release

Using the patchwise model for geochemical heterogeneity, the particle surface coverage rate of the porous matrix is given by [Johnson *et al.*, 1996]

$$\frac{\partial \theta}{\partial t} = \lambda \frac{\partial \theta_f}{\partial t} + (1 - \lambda) \frac{\partial \theta_u}{\partial t}. \quad (5)$$

When considering the dynamic aspects of particle deposition and release, the rate equations corresponding to the favorable and unfavorable surface fractions can be expressed as

$$\frac{\partial \theta_f}{\partial t} = \pi a_p^2 k_{\text{dep},f} n B(\theta_f) - k_{\text{det},f} \theta_f R(\theta_f), \quad (6a)$$

$$\frac{\partial \theta_u}{\partial t} = \pi a_p^2 k_{\text{dep},u} n B(\theta_u) - k_{\text{det},u} \theta_u R(\theta_u), \quad (6b)$$

where the subscripts f and u represent the favorable (λ) and unfavorable ($1 - \lambda$) REV surface fractions, respectively, k_{dep} is the colloid deposition rate coefficient, k_{det} is the colloid release rate coefficient, and $B(\theta)$ and $R(\theta)$ are the dynamic blocking and release functions, respectively. The colloid deposition rate coefficient is related to the single collector efficiency η commonly used in filtration theories by [Johnson and Elimelech, 1995]

$$k_{\text{dep}} = \eta \varepsilon V / 4 = \alpha \eta_0 \varepsilon V / 4, \quad (7)$$

where V is the colloid (or fluid) advection velocity, ε is the porosity of the porous medium, α is the collision efficiency, and η_0 is the favorable single collector removal efficiency.

The dynamic blocking function $B(\theta)$ characterizes the probability of colloid deposition by quantifying the fraction of collector surface still available for deposition of colloids [Johnson and Elimelech, 1995]. It accounts for the blocking effect of deposited colloids on the particle deposition rate. Two types of dynamic blocking functions are generally recognized: the Langmuirian dynamic blocking function and the random sequential adsorption (RSA) dynamic blocking function. Recent experimental investigations have shown that the RSA model describes the dynamics of particle deposition in porous media better than the conventional Langmuirian model [Johnson and Elimelech, 1995; Johnson et al., 1996].

The general form of the RSA dynamic blocking function is

$$B(\theta) = 1 - a_1 \left(\frac{\theta}{\theta_{\text{max}}} \right) + a_2 \left(\frac{\theta}{\theta_{\text{max}}} \right)^2 + a_3 \left(\frac{\theta}{\theta_{\text{max}}} \right)^3, \quad (8)$$

where θ_{max} is the maximum attainable surface coverage and a_1 , a_2 , and a_3 are virial coefficients that can be evaluated theoretically (for ideal particles and collector surfaces) or empirically. The coefficients used by Johnson and Elimelech [1995] for $B(\theta)$ will be used in this colloid transport model as they were found adequate to describe the dynamics of blocking in flow of monodisperse submicrometer-size latex colloids in columns packed with spherical uniform glass beads.

Because we assume that colloid deposition onto the favorable surface fraction is irreversible (i.e., particles and favorable patches are oppositely charged), the RSA model can be used to describe the dynamics of particle deposition onto the favorable surface fraction. A similar dynamic blocking function was also chosen to describe the blocking of the unfavorable fraction, although the deposition onto the unfavorable surface fraction was assumed to be reversible. This assumption, however, has a negligible effect on the colloid transport behavior since the deposition rate on the unfavorable surface fraction is much smaller than that on the favorable fraction, and the maximum surface coverage for the unfavorable surface fraction is much smaller than that on the favorable surface fraction.

The dynamic release function describes the probability of colloid release from porous media surfaces covered by retained colloids, somewhat analogous to the dynamic blocking function. In principle, this function should depend on the colloid residence time and the retained colloid concentration

[Meinders et al., 1992; Johnson et al., 1995]. When $R(\theta) = 1$, the release terms in (6) represent a first-order kinetics release mechanism. Because the mechanisms of colloid release are relatively not as well understood as particle deposition at the present time, only a first-order release rate will be considered in this paper. In all available work on colloid release a first-order colloid release mechanism with either one first-order colloid release rate coefficient or a distribution of first-order release rate coefficients is adopted [e.g., Kallay and Matijevic, 1987; Ryan and Elimelech, 1996; Kretzschmar et al., 1999; Grolmund and Borkovec, 1999].

To summarize, the model for colloid deposition and release is formulated in its most general form to include both colloid deposition and release processes from the favorable as well as the unfavorable surface fractions. Barring changes in solution chemistry, colloid deposition onto the favorable surface fraction is irreversible because particles and favorable patches are oppositely charged so that particles are captured in a deep primary minimum [e.g., Ryan and Elimelech, 1996; Johnson et al., 1996]. The deposition on the unfavorable surface fraction, however, is reversible because both the particles and the unfavorable surface fraction are negatively charged and particles are trapped in a finite and often shallow primary well [e.g., Kallay and Matijevic, 1987; Ryan and Elimelech, 1996; Kretzschmar et al., 1999]. In the simulations presented in this paper, it is assumed that there is no particle release from the favorable surface fraction (i.e., $k_{\text{det},f} = 0$).

2.5. Numerical Solution of the Forward Problem

In this colloid transport model the transient flow equation is coupled with the colloid transport equation. Numerical solution of the colloid transport model can be obtained with both transient and steady state flow fields using the multiple cell balance (MCB) method [Sun, 1995]. The detailed MCB formulation and numerical solution as well as validation of the numerical code are presented by Sun [1998]. Numerical simulations showed that colloidal transport is significantly affected by one hydrologic parameter, the hydraulic conductivity (K), and five transport parameters, namely, the longitudinal dispersivity (α_L), the geochemical heterogeneity (λ), the favorable (fast) colloid deposition rate coefficient ($k_{\text{dep},f}$), the unfavorable (slow) colloid deposition rate coefficient ($k_{\text{dep},u}$), and the colloid release rate coefficient from the unfavorable surface fraction ($k_{\text{det},u}$). Hence it is of paramount importance to systematically investigate the identifiability of these six model parameters.

3. Inverse Problem of Colloid Transport

The objective of the inverse problem is to identify the unknown model parameters from observations of the state variables, which are generally obtained from independent experiments. In the present case the hydraulic head and colloid or solute (tracer) concentration are the pertinent state variables, while the six parameters outlined in section 2 constitute the unknown model parameters.

3.1. Mathematical Formation of the Inverse Problem

It is assumed that the flow field is in steady state and that size exclusion does not influence the colloid advective velocity and dispersion coefficient. The latter is valid for sandy aquifers where the solid matrix pore size is several orders of magnitude larger than the colloid size. Thus, for a given porous medium,

the colloid dispersion coefficient is assumed to be similar to the solute (tracer) dispersion coefficient. On the basis of the above assumptions the inverse problem is separated into two stages. In stage 1 the hydraulic conductivity and longitudinal dispersivity are identified using the flow and tracer transport equations. The other colloid transport parameters are then identified in stage 2, using the colloid transport equation and the parameters found in stage 1.

In stage 1 a coupled inverse problem is solved following these four steps. First, it is assumed that N observations of water head \mathbf{h}^* and $M1$ observations of tracer concentration \mathbf{C}^* , at given times and locations, are known:

$$\mathbf{h}^* = (h_1^*, h_2^*, \dots, h_N^*)^T, \quad (9)$$

$$\mathbf{C}^* = (C_{11}^*, C_{21}^*, \dots, C_{M1}^*)^T. \quad (10)$$

Second, the relationship between state variables (\mathbf{h} and \mathbf{C}) and model parameters (\mathbf{p}) is represented by the numerical model, (1), (3), and (5), with the deposition and release terms absent from the transport equation. The vector \mathbf{p} is the L -dimensional vector of the unknown model parameters:

$$\mathbf{p} = (p_1, p_2, \dots, p_L)^T. \quad (11)$$

In stage 1, $L = 2$, and \mathbf{p} includes one hydrologic parameter (K) and one tracer transport parameter (α_L). By using the given parameter set \mathbf{p} , the simulation model can provide model solutions corresponding to the known observations. These model solutions can be expressed as

$$\mathbf{h}(\mathbf{p}) = \{h_1(\mathbf{p}), h_2(\mathbf{p}), \dots, h_N(\mathbf{p})\}^T \quad (12)$$

$$\mathbf{C}(\mathbf{p}) = \{C_1(\mathbf{p}), C_2(\mathbf{p}), \dots, C_{M1}(\mathbf{p})\}^T. \quad (13)$$

Third, there may be some prior information on the unknown parameters, which is generally the range of the parameter values. Thus an admissible set P_{ad} of \mathbf{p} based on the parameter range can be defined

$$P_{\text{ad}} = \{\mathbf{p} | p_i \leq p_i \leq \bar{p}_i, \quad i = 1, 2, \dots, L\}^T, \quad (14)$$

where p_i and \bar{p}_i are the lower and upper bounds of the i th parameter. Finally, the coupled inverse problem in the first stage is to find a $\mathbf{p}^* \in P_{\text{ad}}$ such that the model output $\mathbf{C}(\mathbf{p}^*)$ and $\mathbf{h}(\mathbf{p}^*)$ are "closest" to the observations of \mathbf{C}^* and \mathbf{h}^* .

In the second stage a relatively simpler inverse problem is at hand. In this stage the unknown parameters are estimated from one state variable: the colloid concentration. The inverse problem is structured as follows. First, it is assumed that there are $M2$ observations of colloid number concentration \mathbf{n}^* over a specified domain in time and space:

$$\mathbf{n}^* = (n_{11}^*, n_{21}^*, \dots, n_{M2}^*)^T. \quad (15)$$

Then, the unknown colloid deposition and release parameters are expressed as a vector of finite dimension, like equation (11), with $L \leq 4$. The relationship between the state variable \mathbf{n} and the model parameters \mathbf{p} is given by the colloid transport equations (3) and (5). The model solution for the given parameter set \mathbf{p} is expressed as

$$\mathbf{n}(\mathbf{p}) = \{n_1(\mathbf{p}), n_2(\mathbf{p}), \dots, n_{M2}(\mathbf{p})\}. \quad (16)$$

Furthermore, an admissible set P_{ad} of \mathbf{p} may also be defined as in equation (14). Finally, the inverse problem in the second stage is to find a $\mathbf{p}^* \in P_{\text{ad}}$, such that the model output, $\mathbf{n}(\mathbf{p}^*)$, is "closest" to the observations \mathbf{n}^* .

3.2. Solution of the Inverse Problem

In the two stages outlined above, the solutions of both inverse problems are composed of three components: the performance function, a search algorithm, and the forward solution of the model. The MCB method was used to obtain the forward solution of both the tracer and colloid transport problems, as described in detail by Sun [1998]. The relevant performance functions and search algorithms are described in sections 3.2.1–3.2.3.

3.2.1. Performance functions. The performance function for the coupled inverse problem in stage 1 can be described in a general form by [Sun, 1994]

$$E = W_h \sum_{n=1}^N w_n (h_n(\mathbf{p}) - h_n^*)^2 + W_c \sum_{m1=1}^{M1} w_{m1} (C_{m1}(\mathbf{p}) - C_{m1}^*)^2, \quad (17)$$

where W_h and W_c are the weighting factors for water head and tracer concentration information, respectively, \mathbf{p} is the identified parameter vector, $h_n(\mathbf{p})$ and h_n^* are the model solution and the observation of water head, respectively, at the n th given location and time, $C_{m1}(\mathbf{p})$ and C_{m1}^* are the model solution and observation of tracer concentration, respectively, at the $m1$ th given location and time, and w_n and w_{m1} are weighting factors for each observation. These weighting factors can be expressed as

$$w_i = 1/\sigma_i^2, \quad i = 1, \dots, I, \quad (18)$$

where σ_i is the standard deviation of the measurement error of the i th observed data point, i represents n or $m1$, and I refers to N or $M1$.

In this study, a 1 m by 3 m confined porous medium was investigated, with the scale being so-called local scale [Sun, 1995]. Owing to the small hydraulic gradient and the rather small scale the maximum change in the hydraulic head within the selected flow field may be smaller than the accuracy of standard measuring techniques, thus making the use of hydraulic head information for parameter identification unrealistic. Furthermore, recent studies indicate that tracer concentration data may be sufficient for identification of the statistical structure of spatially varying parameters or the actual value of a parameter at a given location in a subsurface porous medium [Rubin and Ezzedine, 1997]. Consequently, we use the tracer concentration data solely to identify the two parameters in stage 1 (i.e., K and α_L) and substitute $W_h = 0$ and $W_c = 1$ in (17). Hence the performance function for stage 1 reduces to

$$E = \sum_{m1=1}^{M1} w_{m1} (C_{m1}(\mathbf{p}) - C_{m1}^*)^2. \quad (19)$$

In the second stage the identified parameters from stage 1 are incorporated into the colloid transport model. The performance function for the inverse problem in this stage involves only colloid number concentration:

$$E = \sum_{m2=1}^{M2} w_{m2} (n_{m2}(\mathbf{p}) - n_{m2}^*)^2. \quad (20)$$

Here $n_{m2}(\mathbf{p})$ is the model solution generated by using the estimated model parameters \mathbf{p} , n_{m2}^* is the observed colloid

number concentration, and the weighting factor for each observation, w_{m2} , is defined as in (18).

3.2.2. Search algorithm: The Gauss-Newton-Levenberg-Marquardt method. In both stages the Levenberg-Marquardt modification for the Gauss-Newton method was used to search for the optimal solution. Assuming that the estimated parameter set at the $(i + 1)$ th iteration is \mathbf{p}_{i+1} and the old (i th iteration) estimated parameter set is \mathbf{p}_i , \mathbf{p}_{i+1} then can be expressed as

$$\mathbf{p}_{i+1} = \mathbf{p}_i + \Delta \mathbf{p}_i, \quad (21)$$

where $\Delta \mathbf{p}_i$ is the searching step size. The Gauss-Newton-Levenberg-Marquardt method defines $\Delta \mathbf{p}_i$ by [Sun, 1994]

$$\Delta \mathbf{p}_i = -(\mathbf{A}_i^T \mathbf{A}_i + \mu \mathbf{I})^{-1} \mathbf{A}_i^T \mathbf{f}_i, \quad (22)$$

where \mathbf{I} is the identity matrix and μ is the Levenberg-Marquardt parameter. Note that when $\mu = 0$, the method reduces to the Gauss-Newton method. The matrix \mathbf{A} is the product of the weighting factor matrix \mathbf{W} and the Jacobian matrix \mathbf{J} (also called the sensitivity matrix), the components of the latter being

$$J(j, k) = [\partial U_j / \partial p_k]_{j=1, 2, \dots, M; k=1, 2, \dots, L}. \quad (23)$$

Here U represents the state variables, that is, C (tracer concentration) in the stage 1 and n (colloid concentration) in stage 2; M is the total number of observations; and L is the dimension of the vector \mathbf{p} ($L = 2$ in stage 1 and $L \leq 4$ in stage 2). The expressions for the vector \mathbf{f} for stage 1 and 2 are

$$\mathbf{f}_i(\mathbf{p}_i) = w_i(C_i(\mathbf{p}_i) - C_i^*), \quad (24a)$$

$$\mathbf{f}_i(\mathbf{p}_i) = w_i(n_i(\mathbf{p}_i) - n_i^*), \quad (24b)$$

respectively.

3.2.3. Numerical code. A program was developed to provide the inverse solution. The main procedures and steps in the computer program are the following:

1. Initially guess the values of the unknown model parameters, solve the forward problem, and calculate the value of the performance function to initiate the iteration for the inverse problem.

2. Calculate the searching step size for the parameters (equation (22)) and update the old parameter estimates (equation (21)).

3. Substitute the updated parameters into the model, then solve the forward problem and recalculate the performance function.

4. Compare the new performance function value with the old performance function result. When the value of the performance function decreases with updating the model parameters, the updated model parameter set is taken as one possible solution of the inverse problem, and the iteration is counted as one successful iteration; step 5 is then carried out. Otherwise, the Levenberg-Marquardt parameter (μ in (22)) is adjusted and steps 2–4 are repeated. Each repeated run here is counted as one Levenberg-Marquardt modification. The Levenberg-Marquardt modification is repeated until a successful iteration is reached or the maximum predetermined number of the modifications is reached. When the number of the Levenberg-Marquardt modifications exceeds the predetermined maximum number, the program is terminated and step 5 is skipped. Because the newly updated parameters cannot lower the value of the performance function, the results of the previous successful iteration are set as the final estimates.

5. Repeat steps 2–4 to perform the next successful iteration until the maximum number of such iterations is reached. The final possible inverse solutions are regarded as the estimates of the model parameters.

In the present study, the inverse solution has been generally obtained within eight successful iterations, and the Levenberg-Marquardt modification was carried out no more than 8 times per iteration.

3.3. Identifiability of Model Parameters

When we use the least squares performance to identify a parameter, the parameter must be identifiable in a certain sense. The identifiability of a parameter depends not only on the uniqueness and stability of the inverse solution but also on the quantity and quality of the observation data. Various definitions of parameter identifiability of a distributed parameter system can be found in the literature. The least squares identifiability defined by *Chavent* [1987] is often used because it considers the effect of measurement error. A parameter is said to be least squares identifiable if the least squares performance function for identifying the parameter has a unique minimization in a given region and if the minimization is continuously dependent on the measurement errors. It is difficult to directly verify the sufficient conditions of least squares identifiability presented by *Chavent* [1987]. For a specific problem, however, we may test the identifiability of model parameters by conducting additional inverse solutions. For example, if we use different initial guesses of model parameters to solve the inverse problem and find that the identified parameters always converge to the same values, we may believe that the least squares criterion has a unique global minimization. To verify the continuous dependence, we can add errors to the observation data to solve the inverse problem and see if the identified parameters converge to the same values when the observation errors tend to zero.

In this study, we predetermine a set of parameter values as the “true” parameters and find out if they can be identified. First, the following error-free “observation” data can be obtained from the simulation model:

$$C_{m1}^* = C_{m1}(\mathbf{p}^t) \quad m1 = 1, 2, \dots, M1, \quad (25a)$$

$$n_{m2}^* = n_{m2}(\mathbf{p}^t) \quad m2 = 1, 2, \dots, M2, \quad (25b)$$

where \mathbf{p}^t represents the “true” parameters. Substituting (25a) and (25b) into (19) and (20), respectively, and arbitrarily selecting a set of parameter values as the initial guess to start the iteration process of parameter identification, the search series will converge to a point \mathbf{p} in the parameter space as the identified parameters. The first requirement of identifiability is that all search series must converge to the same point $\mathbf{p} = \mathbf{p}^t$ regardless of the starting point.

Next, random measurement errors are added to the simulated observation data:

$$C_{m1}^* = C_{m1}(\mathbf{p}^t) \pm \sigma_{m1} \nu \quad m1 = 1, 2, \dots, M1, \quad (26a)$$

$$n_{m2}^* = n_{m2}(\mathbf{p}^t) \pm \sigma_{m2} \nu \quad m2 = 1, 2, \dots, M2, \quad (26b)$$

where ν represents the standard Gaussian random variable with zero mean and unit standard deviation and σ_{m1} and σ_{m2}

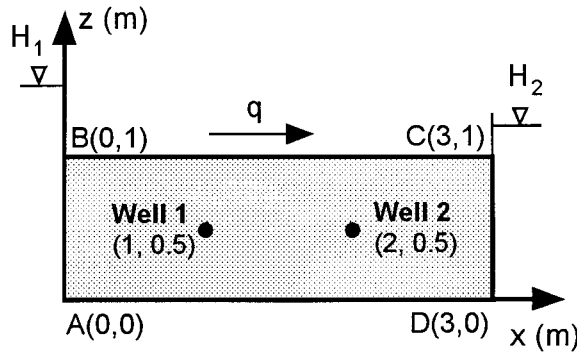


Figure 1. The rectangular model confined aquifer (1 m \times 3 m) with the two sampling wells (1 and 2) used for the present investigation. The z axis represents the vertical direction, and the x axis coincides with the horizontal flow direction. H_1 and H_2 represent the given water level (head) at the two boundaries \overline{AB} and \overline{CD} , respectively, and \mathbf{q} is the Darcy velocity.

are the standard deviations of the observation errors added to C_{m1}^* and n_{m2}^* , respectively. In this study, we use the relative error r to define these standard deviations, i.e., $\sigma_{m1} = rC_{m1}(\mathbf{p}^t)$ and $\sigma_{m2} = rC_{m2}(\mathbf{p}^t)$. The inverse problem is solved for different r values and different realizations of ν . The second requirement of identifiability is that the identified parameters \mathbf{p} are very close to their true values \mathbf{p}^t for all cases when r is small and that \mathbf{p} tends to \mathbf{p}^t when r tends to zero. Generally, to test the identifiability of all parameters in a given range, we need to repeat the above procedure for more \mathbf{p}^t in the range.

4. Sensitivity Analysis

A sensitivity analysis is carried out to gain more information about our colloid transport model prior to parameter identification. Here the transient process of colloid or tracer transport in a steady state fluid flow field is investigated. For such a system the sensitivity coefficient with respect to a parameter as a function of time and observation location is defined by [e.g., Tomovic, 1963],

$$u_{p_i}(t, x, z) = \frac{\partial U(t, p_1, p_2, \dots, p_i, \dots, p_L)}{\partial p_i}, \quad (27)$$

where t is the time, x and z are the coordinates of the observation location, p_i is the i th parameter in the L -dimensional parameter vector \mathbf{p} , with $i = 1, 2, \dots, L$, U is a state variable representing either C or n , and u_{p_i} is the sensitivity coefficient of model parameter p_i .

Because the values of the model parameters may vary over several orders of magnitude for a given observation location, a dimensionless sensitivity coefficient was used to compare the role of the various model parameters [Kokotovich, 1964; Cruz and Perkins, 1973; Kreindler, 1968]:

$$S_{p_i}(t) = \frac{\partial(\ln U)}{\partial(\ln p_i)}. \quad (28)$$

When the perturbation of the model parameter (p_i) is finite, $S_{p_i}(t)$ is obtained as follows [e.g., Cruz and Perkins, 1973]:

$$S_{p_i}(t) = \frac{\Delta U(t, p_1, p_2, \dots, p_i, \dots, p_L)/U_0}{(\Delta p_i/p_i)} \quad (29)$$

$$= \frac{U^*(t, p_1, p_2, \dots, p_i + \Delta p_i, \dots, p_L) - U^*(t, p_1, p_2, \dots, p_i, \dots, p_L)}{(\Delta p_i/p_i)},$$

where S_{p_i} is the dimensionless sensitivity coefficient of parameter p_i , Δp_i is a small perturbation of parameter p_i near its basic value, and U^* is the dimensionless state variable (i.e., C/C_0 or n/n_0).

In the sensitivity analysis presented here, the dimensionless sensitivity coefficient is plotted as a function of observation time for each model parameter at a given observation location to form a sensitivity curve. We first observe the influence of each of the six model parameters on the system and deduce the possible effect of proposed experimental designs on parameter identification. We then estimate the influence of the parameter values on the sensitivity results and deduce the limits within which the model parameters may be identified.

4.1. Dimensionless Sensitivities of Model Parameters

We consider colloid transport in a two-dimensional, vertical, and confined aquifer. Initially, the aquifer contains no colloids. The flow region (Figure 1) is a rectangle (1 m \times 3 m) with given head (H_1) and colloidal concentration (n_0) at boundary \overline{AB} , given head (H_2) and zero colloid dispersive flux at boundary \overline{CD} , and no-flow condition at boundaries \overline{AD} and \overline{BC} . The tracer or colloid breakthrough curves (BTCs) are collected at observation well 1 ($x = 1.0$ m and $z = 0.5$ m).

Six key model parameters were investigated: hydraulic conductivity (K), longitudinal dispersivity (α_L), geochemical heterogeneity (λ), favorable colloid deposition rate coefficient ($k_{\text{dep},f}$), unfavorable colloid deposition rate coefficient ($k_{\text{dep},u}$), and colloid release rate coefficient from unfavorable surface fraction ($k_{\text{det},u}$). The basic values and ranges of the investigated parameters (Table 1) are representative of previous field observation data, and most are typical of sandy aquifers [e.g., Gelhar et al., 1992; McCarthy and Degueudre, 1993; Ryan et al., 1999].

Considering the case of long colloid injection (duration of 10 days), the dimensionless sensitivities of the key model parameters calculated from (29) are shown in Figure 2. Three main features can be seen in these results. First, the dimensionless sensitivities are quite different in magnitude, thus pointing out the difficulty in identifying all the model parameters as a group. Second, the six parameters can be listed in a decreasing order of their maximum dimensionless sensitivity values as $S_K > S_\lambda > S_{k_{\text{det},f}} > S_{\alpha_L} > S_{k_{\text{dep},u}} > S_{k_{\text{det},u}}$. Third, the various regions in the colloid BTC are not equally sensitive to all model parameters. The ascending and descending portions of the BTC are highly sensitive to both hydraulic conductivity and longitudinal dispersivity (Figure 2d). Furthermore, the front of the BTC is sensitive to geochemical heterogeneity and favorable colloid deposition rate coefficient (Figure 2b), whereas the tail of the BTC is more sensitive to the colloid release rate coefficient from the unfavorable surface fraction than the other parameters (Figure 2c).

A relatively short colloid injection duration (0.5 days) was also used to produce observation data. This short injection

Table 1. Basic Values and Ranges of the Parameters Used in the Sensitivity Analysis and Parameter Identification

Parameter	Basic Value	Range
Hydraulic conductivity K , m d^{-1}	100	30–150
Specific storage S_s	0.0001	
Porosity ε	0.4	
Grain radius a_c , mm	0.15	
Particle radius a_p , μm	0.15	
Longitudinal dispersivity α_L , m	0.05	0.01–0.5
Transverse dispersivity α_T , m	0.2 α_L	
Geochemical heterogeneity λ	0.01	10^{-4} – 10^{-1}
Favorable (fast) deposition rate coefficient $k_{\text{dep},f}$, m d^{-1}	6.5×10^{-3}	10^{-4} – 10^{-1}
Unfavorable (slow) deposition rate coefficient $k_{\text{dep},u}$, m d^{-1}	6.5×10^{-6}	10^{-8} – 10^{-3}
Release rate from favorable fraction $k_{\text{det},f}$, d^{-1}	0.0	
Release rate from unfavorable fraction $k_{\text{det},u}$, d^{-1}	5×10^{-4}	10^{-8} – 10^{-3}
Maximum attainable surface coverage θ_{max}	0.2	
Particle number concentration n_0 , m^{-3}	2.8×10^{14}	
Particle mass concentration C_0 , mg L^{-1}	10.8	

results in a pulse-like colloid breakthrough curve. The dimensionless sensitivity values of the four colloid transport parameters are shown in Figure 3. Comparing Figures 2 and 3 clearly demonstrates that the pulse-like colloid BTC nearly eliminates the possibility of estimating the colloid release rate coefficient from the unfavorable surface fraction. However, short injection duration does not affect the dimensionless sensitivities of the geochemical heterogeneity, the favorable colloid deposition rate coefficient, and the unfavorable colloid deposition rate coefficient. This feature implies that only those parameters representing the rapid kinetics processes (i.e., colloid deposition in the present case) may be estimated from pulse-like colloid BTCs. To identify the parameters controlling the relatively slow kinetics process (i.e., colloid release in the present case) simultaneously, a sufficiently long injection duration is required.

4.2. Effect of Parameter Values on Dimensionless Sensitivity

In this section we consider the effect of parameter values on the dimensionless sensitivity results. By fixing all other model parameters, the BTCs and the corresponding dimensionless sensitivity curves with respect to different basic values of a single colloid deposition or release parameter (i.e., λ , $k_{\text{dep},f}$, or $k_{\text{det},u}$) are plotted in Figures 4–6.

Inspection of these results reveals that the effect of parameter values on the relative sensitivity is quite different for the various model parameters. When geochemical heterogeneity (λ) changes from $O(10^{-3})$ to $O(10^{-1})$, its dimensionless sensitivity values increase from almost 0 to a value greater than 1 (Figure 4). By assuming a fixed collision efficiency (a ratio of $k_{\text{dep},u}$ to $k_{\text{dep},f}$) of 10^{-3} , an increase in the rate constant for favorable deposition ($k_{\text{dep},f}$) decreases the dimensionless sensitivity of this parameter (Figure 5). Finally, the dimensionless sensitivity of the colloid release rate coefficient from the unfavorable surface fraction ($k_{\text{det},u}$) increases with an increase in the parameter values (Figure 6). Generally, the larger the sensitivity coefficient of a model parameter is, the higher is the likelihood for the parameter to be identified. After setting up reasonable criteria for dimensionless sensitivity, we expect to estimate the limits of parameter value within which the parameter may be identified.

The dimensionless sensitivity coefficients were obtained by assuming that the values of the rest of the model parameters

are known and fixed. In the proposed model the colloid deposition rate coefficients (both favorable and unfavorable), the geochemical heterogeneity, and the dynamic blocking function all affect the overall process of particle deposition, while the geochemical heterogeneity, the unfavorable colloid deposition rate coefficient, and the colloid release rate coefficient control the apparent colloid release. Because the shape of the colloid BTCs is determined by the processes of colloid deposition and release, it is very likely that the sensitivity of a model parameter is also affected by the basic values of other parameters. When more than one parameter changes in such a system, the effect of parameter values on the sensitivity results of all the model parameters is expected to be more complicated, and it becomes harder to estimate the value limits within which model parameters may be identified.

5. Parameter Identifiability

In the identifiability of the model parameters the basic values of the six model parameters (Table 1) are set as the true parameter values. On the basis of those true parameter values the breakthrough curves (BTCs) at observation well 1 (Figure 1) were simulated with or without random error and served as observation data for most of the results shown. The hydraulic conductivity and longitudinal dispersivity were estimated from the solute tracer data; these were taken as known parameters to identify the other four colloid deposition and release parameters from colloid BTC data.

5.1. Identification of Hydraulic Conductivity and Longitudinal Dispersivity

Hydraulic conductivity and longitudinal dispersivity were identified together from the tracer BTCs with injection duration of 0.5 days. The investigation of parameter identification was divided into two steps. First, the uniqueness of the inverse solution was studied using error-free observation data. Second, the identifiability of the two-parameter vector was studied in the presence of random observation errors.

In the first step a parametric phase space given by $30 \leq K \leq 150 \text{ m d}^{-1}$ and $0.01 \leq \alpha_L \leq 0.5 \text{ m}$ was explored. Starting from different initial guesses of the parameter vector (K , α_L), namely, (30, 0.01), (80, 0.1), and (150, 0.5), minimization runs were carried out to check if the model parameters attain the true values of (100, 0.05). Different initial guesses led to similar

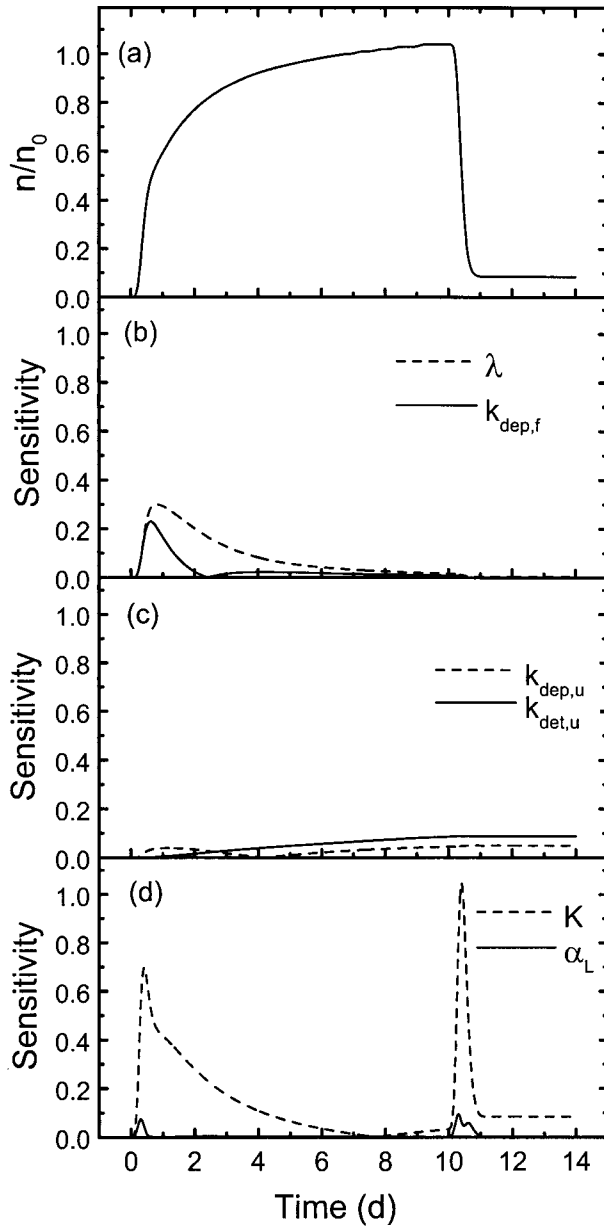


Figure 2. The dimensionless sensitivity of the six model parameters (injection duration of 10 days). (a) The particle breakthrough curve observed in sampling well 1. The remaining plots are the corresponding sensitivity curves for (b) λ and $k_{\text{dep},f}$, (c) $k_{\text{dep},u}$ and $k_{\text{det},u}$, and (d) K and α_L . The basic parameter values are $K = 100.0 \text{ m d}^{-1}$, $\lambda = 0.01$, $k_{\text{dep},f} = 6.5 \times 10^{-3} \text{ m d}^{-1}$, $k_{\text{dep},u} = 6.5 \times 10^{-6} \text{ m d}^{-1}$, $k_{\text{det},u} = 5.0 \times 10^{-4} \text{ d}^{-1}$, and $\alpha_L = 0.05 \text{ m}$.

end points which converged to the true parameter values with relative errors $\leq 0.01\%$ for K and $\leq 1.6\%$ for α_L . The results show that within the limited number of trials conducted, the performance function is convex and has a unique minimum within the selected range of the parametric phase space.

In the second step, two different relative observation errors (5% and 10%) were chosen to simulate the observation data (equation (26)). For each relative observation error the observation data were simulated 10 times, and the hydraulic conductivity and longitudinal dispersivity were identified together

from these observation data. The average estimated values, the sample standard deviations of the estimates, the coefficients of variation, and the relative estimation errors were then calculated for these ten sets of estimates (Table 2). As shown, the average estimated values of both hydraulic conductivity and longitudinal dispersivity are very close to their true values. The small coefficients of variation of both parameters are indicative of the good quality of these estimations. The relative estimation errors (0.1% for K and 18.0% for α_L) are small enough when considering a relative observation error of 10%. When the observation error is reduced (5%), the estimation error is even smaller (0% for K and 8.0% for α_L). The least squares identifiability requires that the identified parameters tend to the original parameters when the observation error tends to zero. Hence the proposed method is capable of identifying the hydraulic conductivity and longitudinal dispersivity from the tracer BTCs in the sense of least squares identifiability.

5.2. Identification of Colloid Deposition and Release Parameters

5.2.1. Interrelationship between colloid deposition and release parameters. To investigate the uniqueness of the inverse solution for the four colloid deposition and release pa-

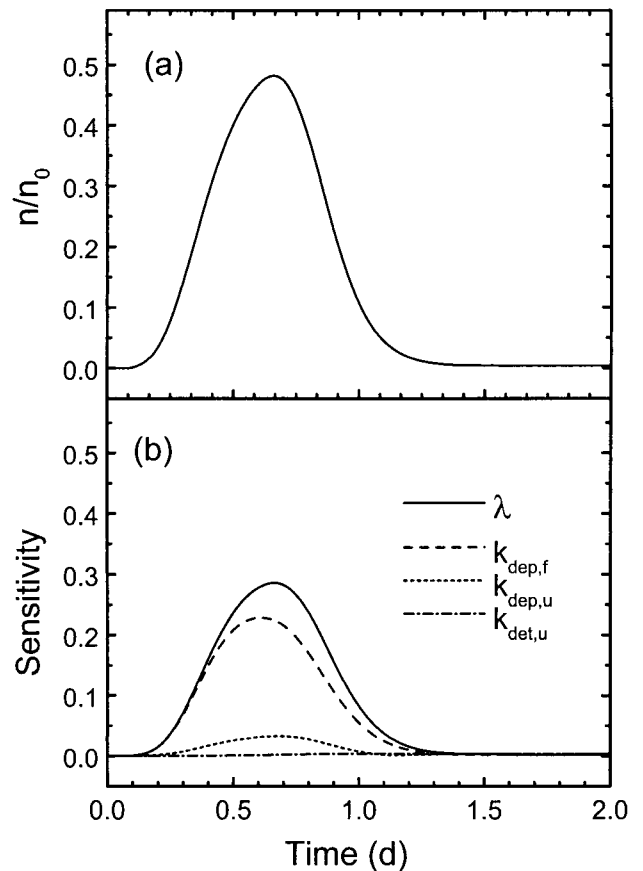


Figure 3. The dimensionless sensitivity of colloid deposition and release parameters for a short colloid injection duration (0.5 days). (a) The particle breakthrough curve observed in well 1. (b) The dimensionless sensitivity curves of λ , $k_{\text{dep},f}$, $k_{\text{dep},u}$, and $k_{\text{det},u}$. The basic values of the model parameters are $K = 100.0 \text{ m d}^{-1}$, $\lambda = 0.01$, $k_{\text{dep},f} = 6.5 \times 10^{-3} \text{ m d}^{-1}$, $k_{\text{dep},u} = 6.5 \times 10^{-6} \text{ m d}^{-1}$, $k_{\text{det},u} = 5.0 \times 10^{-4} \text{ d}^{-1}$, and $\alpha_L = 0.05 \text{ m}$.

rameters, we chose the lower and upper limits for each parameter based on the realistic range of parameter values given in Table 1. Fixing the lower or upper limit of each studied parameter as an initial guess, 16 combinations of such initial guesses were used for estimating the four unknown colloid deposition and release parameters. The inverse solutions were obtained by using error-free observation data. The simulation results show that different initial guesses lead to quite different inverse solutions, which never converge to the true solution. Although initial guesses very close to the true values can reduce the above problem, this requirement is too strict to make the estimation method applicable. Therefore it may be concluded that the group of the four colloid deposition and release parameters does not have a unique inverse solution. Without considering this fact, simple curve fitting methods may provide erroneous parameter values for our colloid transport model or other complex models.

The four colloid deposition and release parameters in the model are closely interrelated. This interrelationship can be verified from the correlation coefficient matrix of these four parameters. First, the covariance matrix of these four model parameters can be estimated by [e.g., Sun, 1994]

$$\text{cov}(\mathbf{p}) \approx \sigma^2 (J^T J)^{-1}, \quad (30)$$

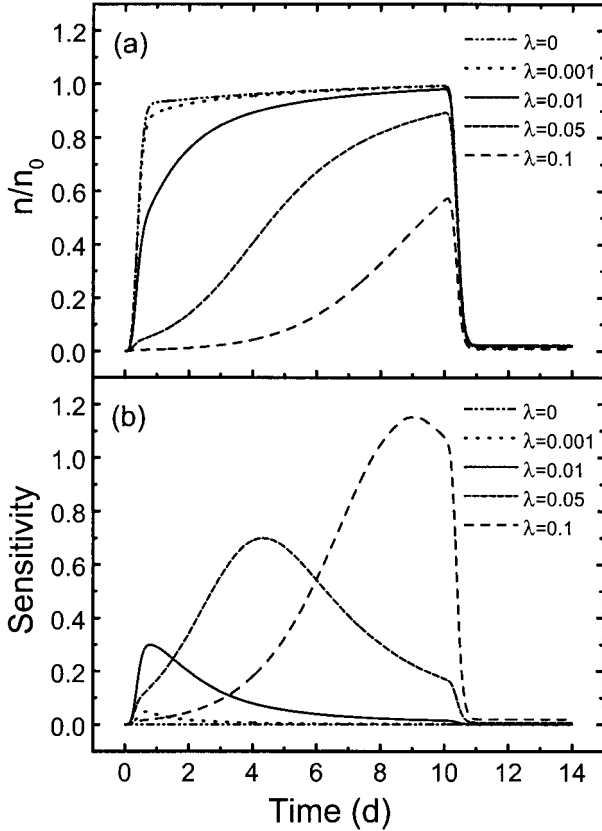


Figure 4. The effect of parameter values of geochemical heterogeneity on its dimensionless sensitivity (injection duration of 10 days): (a) particle breakthrough curves corresponding to five different λ (sampled at well 1) and (b) the corresponding dimensionless sensitivity curves of λ . The other parameters used are listed in Table 1.

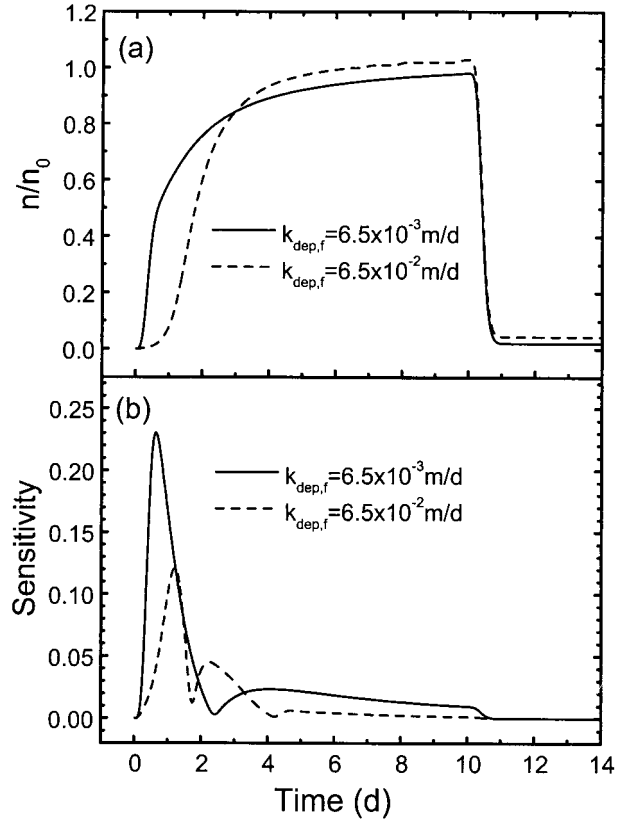


Figure 5. The effect of parameter values of the favorable (fast) colloid deposition rate coefficient on its dimensionless sensitivity (injection duration of 10 days). The collision efficiency is 10^{-3} . (a) The particle breakthrough curves corresponding to the different $k_{\text{dep},f}$ (sampled at well 1) and (b) the corresponding dimensionless sensitivity curves of $k_{\text{dep},f}$. The other parameters used are listed in Table 1.

where \mathbf{p} is the vector of the studied parameters, σ^2 is the observation error variance, and J and J^T are the Jacobian matrix and its transpose, respectively. The relation between an element of the covariance matrix (a_{ij}) and an element of the correlation coefficient matrix (a_{ij}^*) can be expressed as

$$a_{ij}^* = a_{ij} / \sqrt{a_{ii} a_{jj}}. \quad (31)$$

The correlation coefficient matrix for the four colloid deposition and release parameters is

$$\begin{matrix} \lambda & k_{\text{dep},f} & k_{\text{dep},\mu} & k_{\text{det},\mu} \end{matrix} \begin{bmatrix} \lambda & k_{\text{dep},f} & k_{\text{dep},\mu} & k_{\text{det},\mu} \\ 1.00 & -1.00 & -1.00 & 1.00 \\ -1.00 & 1.00 & 1.00 & -0.99 \\ -1.00 & 1.00 & 1.00 & -0.99 \\ 1.00 & -0.99 & -0.99 & 1.00 \end{bmatrix}. \quad (32)$$

The above matrix clearly shows that the four colloid deposition and release parameters are strongly interrelated. Consequently, it is difficult to identify all these four model parameters simultaneously.

On the basis of the above results the number of studied parameters was reduced to three to obtain a set of parameters that are mutually independent. By using the same experimental design described above, the correlation coefficient matrices

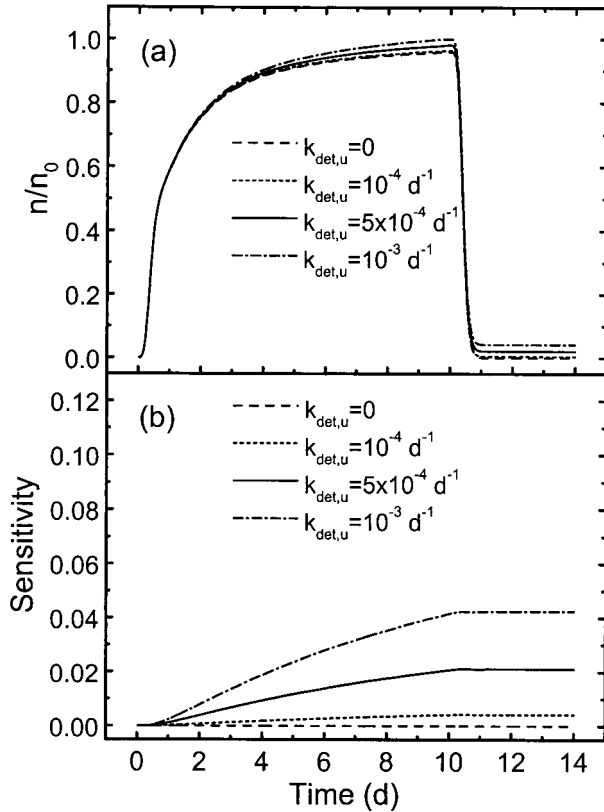


Figure 6. The effect of parameter values of the unfavorable (slow) colloid release rate constant on its dimensionless sensitivity (injection duration of 10 days): (a) the particle breakthrough curves corresponding to the different $k_{\text{det},u}$ (sampled at well 1) and (b) the corresponding dimensionless sensitivity curves of $k_{\text{det},u}$. The other parameters used are listed in Table 1.

for different sets of three colloid deposition and release parameters were obtained:

$$\begin{matrix} \lambda \\ k_{\text{dep},u} \\ k_{\text{det},u} \end{matrix} \begin{bmatrix} \lambda & k_{\text{dep},u} & k_{\text{det},u} \\ 1.00 & -0.94 & 0.47 \\ -0.94 & 1.00 & -0.44 \\ 0.47 & -0.44 & 1.00 \end{bmatrix}, \quad (33a)$$

$$\begin{matrix} k_{\text{dep},f} \\ k_{\text{dep},u} \\ k_{\text{det},u} \end{matrix} \begin{bmatrix} k_{\text{dep},f} & k_{\text{dep},u} & k_{\text{det},u} \\ 1.00 & -0.52 & -0.12 \\ -0.52 & 1.00 & -0.10 \\ -0.12 & -0.10 & 1.00 \end{bmatrix}, \quad (33b)$$

$$\begin{matrix} \lambda \\ k_{\text{dep},f} \\ k_{\text{det},u} \end{matrix} \begin{bmatrix} \lambda & k_{\text{dep},f} & k_{\text{det},u} \\ 1.00 & -0.78 & 0.42 \\ -0.78 & 1.00 & -0.37 \\ 0.42 & -0.37 & 1.00 \end{bmatrix}, \quad (33c)$$

$$\begin{matrix} \lambda \\ k_{\text{dep},f} \\ k_{\text{dep},u} \end{matrix} \begin{bmatrix} \lambda & k_{\text{dep},f} & k_{\text{dep},u} \\ 1.00 & -0.81 & -0.94 \\ -0.81 & 1.00 & 0.67 \\ -0.94 & 0.67 & 1.00 \end{bmatrix}. \quad (33d)$$

The four matrices showed that the correlation coefficients decrease by reducing the number of the identified parameters, and the different combinations of three colloid deposition and release parameters have different degrees of correlation. Fur-

thermore, when either geochemical heterogeneity or one of the colloid deposition rate coefficients is known, the remaining colloid deposition and release parameters are weakly related to each other. Thus, using the present model, three parameters may be identified simultaneously.

5.2.2. Uniqueness of the inverse solution for three-parameter set. As the major settings of subsurface aquatic environments are unfavorable for colloid deposition and the colloid deposition on this large unfavorable surface fraction is often reversible [e.g., *McDowell-Boyer, 1992*], a slow colloid release is very likely to exist simultaneously with colloid deposition. We chose a small colloid release rate coefficient ($5 \times 10^{-4} \text{ d}^{-1}$) to generate the observation data. One of the four colloid deposition and release parameters was assumed to identify the other three parameters. The simulation results show that a unique inverse solution for the three-parameter set can be obtained if either the geochemical heterogeneity or the favorable colloid deposition rate coefficient is known (Table 3). Therefore either λ or $k_{\text{dep},f}$ needs to be known before the other parameters are identified.

In practice, there may be prior information on some model parameters, although no such information was assumed in this study. It is also reasonable to use the calculated favorable colloid deposition rate coefficient based on filtration theory as its estimate because the available expressions for favorable colloid deposition coefficient constant are known to be in reasonable agreement with experimental results [e.g., *Elimelech and O'Melia, 1990; Elimelech et al., 1995*].

5.2.3. Stability of the inverse solution for the three-parameter set. Assuming a known favorable colloid deposition rate coefficient, the stability of the inverse solution for the other three parameters was investigated for a case of long injection. Following the procedure of parameter identification described in section 5.1, the observed data were simulated 10 times, with each set of observation data obtained by incorporating 5% or 10% relative error. The average estimated values and the coefficients of variation of the estimates for the three parameters based on 10 simulations are given in Table 4. Although the values of the three parameters vary in magnitude, the estimated parameter values are close enough to their true

Table 2. Statistical Evaluation of the Estimated Hydraulic Conductivity and Longitudinal Dispersivity Based on Ten Simulations for Each of the Relative Observation Errors (5% or 10%)^a

	Relative Observation Error	
	5%	10%
Average estimated value		
K	100.0 m d ⁻¹	100.1 m d ⁻¹
α_L	0.054 m	0.059 m
Sample standard deviation		
K	0.827 m d ⁻¹	1.779 m d ⁻¹
α_L	0.003 m	0.007 m
Coefficient of variation		
K	0.00827	0.0177
α_L	0.056	0.1186
Relative estimation error (to the true solutions)		
K	0.0%	0.1%
α_L	8.0%	18.0%

^aThe true values of K and α_L are 100.0 m d⁻¹ and 0.05 m, respectively.

Table 3. Uniqueness of the Inverse Solution for Particle Deposition and Release Parameters^a

Parameter	Initial Guess	Estimated Parameter for Given λ	Estimated Parameter for Given $k_{dep,f}$, $m d^{-1}$	True Value
λ	10^{-4}	NR ^b	0.01	0.01
$k_{dep,f}$, $m d^{-1}$	10^{-4}	6.50×10^{-3}	NR	6.50×10^{-3}
$k_{dep,u}$, $m d^{-1}$	10^{-8}	6.50×10^{-6}	6.50×10^{-6}	6.50×10^{-6}
$k_{det,u}$, d^{-1}	10^{-8}	5.00×10^{-4}	5.00×10^{-4}	5.00×10^{-4}
λ	10^{-3}	NR	0.01	0.01
$k_{dep,f}$, $m d^{-1}$	10^{-3}	6.50×10^{-3}	NR	6.50×10^{-3}
$k_{dep,u}$, $m d^{-1}$	10^{-5}	6.50×10^{-6}	6.50×10^{-6}	6.50×10^{-6}
$k_{det,u}$, d^{-1}	10^{-5}	5.00×10^{-4}	5.00×10^{-4}	5.00×10^{-4}
λ	10^{-1}	NR	0.01	0.01
$k_{dep,f}$, $m d^{-1}$	10^{-1}	6.50×10^{-3}	NR	6.50×10^{-3}
$k_{dep,u}$, $m d^{-1}$	10^{-3}	6.50×10^{-6}	6.50×10^{-6}	6.50×10^{-6}
$k_{det,u}$, d^{-1}	10^{-3}	5.00×10^{-4}	5.00×10^{-4}	5.00×10^{-4}

^aInverse solution is based on observation data from well 1.

^bNR (not relevant) indicates the value of the corresponding parameter is known and is equal to its true value. The remaining three values in the same set are the inverse solutions.

values. The BTCs produced by the true parameters and the BTCs predicted by the estimated parameters are compared in Figures 7a and 7b for 5% and 10% observation errors, respectively. The predicted BTC (simulated based on estimated parameters) describes the observation data (containing observation errors) very well, and it is in very close agreement with the true BTC (computed based on the true parameters). Once again, the estimates tend to the true parameter values when the observation error is reduced, indicating that when either λ or $k_{dep,f}$ is known and long injection is applied, the set of the other three colloid deposition and release parameters may be identified in the sense of least squares identifiability.

5.2.4. Effect of injection duration on parameter identification. The sensitivity analysis presented in section 4 revealed that a relatively short injection (0.5 days) masks the role of the

small colloid release rate (Figure 3). In this section the same injection duration (0.5 days) was assumed to investigate the effect of injection duration on parameter identification. For a

Table 4. Identification of Geochemical Heterogeneity, Unfavorable (Slow) Particle Deposition Rate Coefficient, and Particle Release Rate Coefficient From the Unfavorable Surface Fraction^a

	Observation Error	
	5%	10% Average estimated value
λ	1.05×10^{-2}	1.09×10^{-2}
$k_{dep,u}$	$5.14 \times 10^{-6} m d^{-1}$	$4.71 \times 10^{-6} m d^{-1}$
$k_{det,u}$	$6.51 \times 10^{-4} d^{-1}$	$6.77 \times 10^{-4} d^{-1}$
Sample standard deviation		
λ	7.42×10^{-4}	1.40×10^{-3}
$k_{dep,u}$	$2.77 \times 10^{-6} m d^{-1}$	$5.43 \times 10^{-6} m d^{-1}$
$k_{det,u}$	$2.65 \times 10^{-4} d^{-1}$	$3.51 \times 10^{-4} d^{-1}$
Coefficient of variation		
λ	0.07	0.13
$k_{dep,u}$	0.54	1.15
$k_{det,u}$	0.41	0.52
Relative error to the true value		
λ	5.5%	8.6%
$k_{dep,u}$	20.9%	27.5%
$k_{det,u}$	30.2%	35.3%

^aThe favorable (fast) colloid deposition rate constant is known ($6.5 \times 10^{-3} m d^{-1}$). The true values of λ , $k_{dep,u}$, and $k_{det,u}$ are 0.01, $6.5 \times 10^{-6} m d^{-1}$, and $5.0 \times 10^{-4} d^{-1}$, respectively.

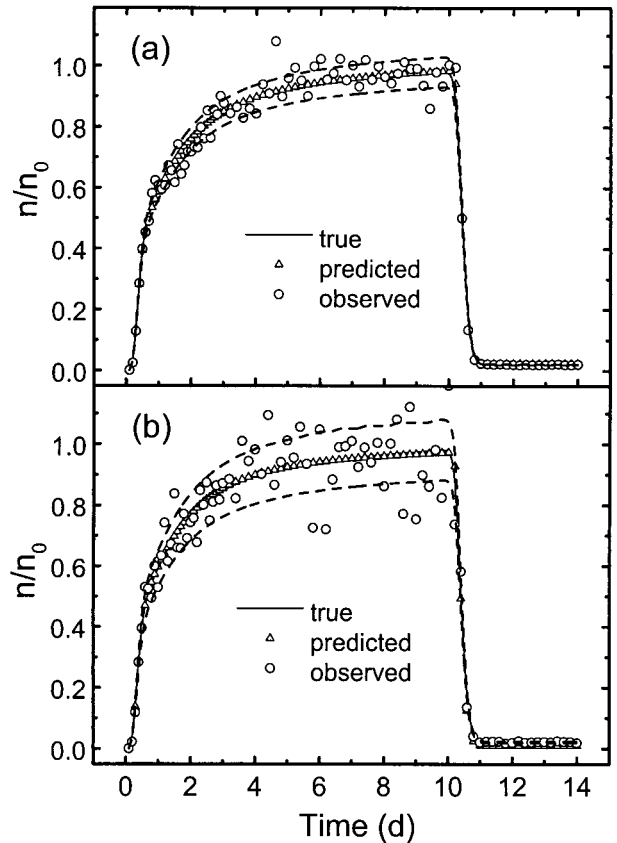


Figure 7. Comparison of simulated observation data (circles), true particle breakthrough curves (solid line), and predicted breakthrough curves (triangles) for (a) relative observation error of 5% and (b) relative observation error of 10%. Most of the simulated observation data fall within 1 standard deviation of the true breakthrough curve (BTC) (between the upper and lower broken lines).

Table 5. Effect of Particle Release Rate on Parameter Identification for a Short Injection Duration^a

	Relative Observation Error					
	0%		5%		10%	
	Case I	Case II	Case I	Case II	Case I	Case II
Average estimated value						
λ	1.02×10^{-2}	1.00×10^{-2}	8.55×10^{-3}	9.53×10^{-3}	8.02×10^{-3}	9.18×10^{-3}
$k_{\text{dep},u}$, m d^{-1}	5.22×10^{-6}	6.51×10^{-6}	1.46×10^{-5}	9.38×10^{-6}	1.80×10^{-5}	1.18×10^{-5}
Sample standard deviation						
λ			2.10×10^{-3}	1.02×10^{-3}	2.86×10^{-3}	6.98×10^{-4}
$k_{\text{dep},u}$, m d^{-1}			1.05×10^{-5}	4.44×10^{-6}	1.48×10^{-5}	5.41×10^{-6}
Coefficient of variation						
λ			2.46×10^{-1}	1.08×10^{-1}	3.56×10^{-1}	7.61×10^{-2}
$k_{\text{dep},u}$			7.21×10^{-1}	4.73×10^{-1}	8.18×10^{-1}	4.58×10^{-1}
Relative error to true value						
λ	2.0%	0.0%	14.5%	4.7%	19.8%	8.2%
$k_{\text{dep},u}$	19.8%	0.1%	124.0%	44.4%	176.9%	81.9%

^aIn case I, $k_{\text{det},u}$ is unknown, and it is ignored in the simulation. In case II, $k_{\text{det},u}$ is known, and it has the value of $5.0 \times 10^{-4} \text{ d}^{-1}$. The favorable colloid deposition rate constant is known ($6.5 \times 10^{-3} \text{ m d}^{-1}$), and the parameters λ and $k_{\text{dep},u}$ are identified for both cases. The true values of λ and $k_{\text{dep},u}$ are 0.01 and $6.5 \times 10^{-6} \text{ m d}^{-1}$, respectively.

colloid release rate coefficient of about 2 orders of magnitude smaller than the colloid deposition rate constant, the simulation results show that a relatively small colloid release rate cannot be identified in the case of a short injection duration. This is consistent with the results of sensitivity analysis shown earlier in Figure 3. Hence experiments should be designed carefully to capture enough information on colloid deposition and release parameters, and sensitivity analyses may provide insights into such experimental designs.

Because short injection duration is widely used in colloid transport experiments, we elaborate here the problems of identifying the model parameters from such experiments. Since the small colloid release rate coefficient cannot be identified from the BTC of short injection, it is very likely to be ignored. To study the discrepancies introduced by such neglect of colloid release, we performed the following calculations. First, the observation data were simulated with inclusion of a small colloid release rate coefficient. Then, we fixed $k_{\text{dep},f}$ and identified λ and $k_{\text{dep},u}$ from the simulated observation data, which are either the error-free BTC data or the BTC data containing 5% or 10% random observation error. The estimates of λ and $k_{\text{dep},u}$ when neglecting $k_{\text{det},u}$ (setting the release rate coefficient to zero), were compared with the inverse solutions by assuming a known $k_{\text{det},u}$ in Table 5.

It is evident that the relative estimation error increases significantly when neglecting the existence of the small colloid release. The relative estimation errors increase from 0.0% to 2.0% for λ and from 0.1% to 19.8% for $k_{\text{dep},u}$ for the case of error-free observation data and increase from 8.2% to 19.8% for λ and from 81.9% to 176.9% for $k_{\text{dep},u}$ for the case of 10% relative observation error (Table 5). However, when the role of the small colloid release was taken into account, the results in Table 5 are comparable with the inverse solution with a long injection duration (Table 4). It can be seen that the short injection duration causes only a slight change in the estimation error in λ (from 8.2% to 8.6%) but causes a relatively larger estimation error in $k_{\text{dep},u}$ (from 27.5% to 81.9%). The estimation error in $k_{\text{dep},u}$ caused by the short injection duration, however, is much smaller than the estimation error introduced by neglecting colloid release.

These “incorrect” model parameters may potentially affect

the prediction of colloid transport. For instance, for a long injection duration of 10 days, the estimated parameters in Table 5 were used to predict colloid BTC in well 2 (2.0 and 0.5 m). The results are shown in Figure 8. Although the predicted BTC can roughly describe the true BTC, a clear discrepancy between the true BTC and the predicted BTCs can be seen in the presence of this rather small simultaneous colloid release rate. To avoid the estimation error introduced by neglecting the small colloid release, experiments with long injection duration are recommended, especially when the effect of

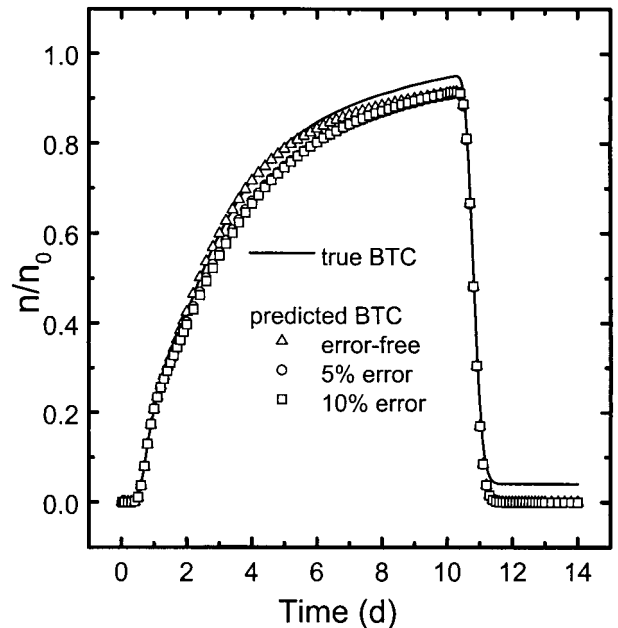


Figure 8. Effect of ignoring the slow colloid release. The particle breakthrough curves are sampled at well 2 ($x = 2.0 \text{ m}$ and $z = 0.5 \text{ m}$). The solid line represents the true BTC, and the symbols are the predicted BTCs when ignoring colloid release. Model parameters were estimated from error-free observation data (triangles), (b) 5% random error (circles), and (c) 10% random error (squares).

colloid release rate constant on parameter identification cannot be ignored or the value of the colloid release rate is desired.

6. Conclusion

The identifiability of six important model parameters of a two-dimensional colloid transport model was investigated. The parameter identification is divided into two steps. The first step involves a coupled inverse problem, where both hydraulic conductivity and longitudinal dispersivity are identified from tracer breakthrough curves. In the second step the estimated parameters from the first step are used in the colloid transport equation, and colloid deposition and release parameters are identified from colloid breakthrough curves. It was found that the four colloid deposition and release parameters are highly interrelated and the inverse solution of the four-parameter set is not unique. When either the geochemical heterogeneity or the favorable (fast) colloid deposition rate coefficient is known, the remaining three colloid deposition and release parameters, namely, favorable colloid deposition rate coefficient (or geochemical heterogeneity), unfavorable (slow) colloid deposition rate coefficient, and colloid release rate coefficient from the unfavorable surface fraction, can be identified. An additional condition is that colloid injection duration is long enough. When injection duration is relatively short, the small colloid release rate coefficient cannot be identified. Ignoring the role of the small colloid release rate results in estimation errors of other model parameters and thus adversely affects the subsequent prediction of colloid transport. The proposed inverse methodology can be extended to colloid transport problems in sandy aquifers where geochemical heterogeneity is controlled by iron oxide coatings. However, complex field-scale effects, which are beyond the scope of this paper, must be considered.

Acknowledgments. The authors acknowledge the support of EPA (cooperative agreement CR824593-01 with R. S. Kerr Laboratory), NSF (grants EAR-9418472 and BES-9705717), and the University of California Water Resources Center (Project W-869).

References

- Bales, R. C., S. R. Hinkle, T. W. Kroeger, K. Stocking, and C. P. Gerba, Bacteriophage adsorption during transport through porous media: Chemical perturbations and reversibility, *Environ. Sci. Technol.*, 25, 2088–2095, 1991.
- Bear, J., *Dynamics of Fluids in Porous Media*, Dover, Mineola, N. Y., 1972.
- Carrera, J., State of the art of the inverse problem applied to the flow and solute transport problems, in *Groundwater Flow and Quality Modeling, NATO ASI Ser., Ser. C*, pp. 549–585, Kluwer Acad., Norwell, Mass., 1998.
- Chavent, G., Identifiability of parameters in the output least square formulation, in *Identifiability of Parametric Models*, edited by E. Walter, Pergamon, Tarrytown, N. Y., 1987.
- Coston, J. A., C. C. Fuller, and J. A. Davis, Pb²⁺ and Zn²⁺ adsorption by a natural aluminum- and iron-bearing surfaces coating on an aquifer sand, *Geochim. Cosmochim. Acta*, 59, 3535–3547, 1995.
- Cruz, J. B., and W. R. Perkins, A new approach to the sensitivity problem in multivariable feedback system design, in *System Sensitivity Analysis*, edited by J. B. Cruz Jr., pp. 125–132, Van Nostrand Reinhold, New York, 1973.
- Elimelech, M., and C. R. O'Melia, Kinetics of deposition of colloidal particles in porous media, *Environ. Sci. Technol.*, 24, 1528–1536, 1990.
- Elimelech, M., J. Gregory, X. Jia, and R. Williams, *Particle Deposition and Aggregation*, Butterworth-Heinemann, Woburn, Mass., 1995.
- Gelhar, L. W., C. Welty, and K. R. Rehfeldt, A critical review of data on field-scale dispersion in aquifers, *Water Resour. Res.*, 28(7), 1955–1974, 1992.
- Ginn, T. R., and J. H. Cushman, Inverse methods for subsurface flow: A critical review of stochastic techniques, *Stochastic Hydrol. Hydraul.*, 4, 1–26, 1990.
- Grolimund, D., and Borkovec, M., Long-term release kinetics of colloidal particles from natural porous media, *Environ. Sci. Technol.*, 33, 4054–4060, 1999.
- Harmand, B., E. Rodier, M. Sardin, and J. Dodds, Transport and capture of submicron particles in a natural sand: Short column experiments and a linear model, *Colloid Surf. A*, 107, 233–244, 1996.
- Harvey, C. F., and S. M. Gorelick, Temporal moment-generating equations: Modeling transport and mass transfer in heterogeneous aquifers, *Water Resour. Res.*, 31(8), 1895–1911, 1995.
- Harvey, R. W., and S. P. Garabedian, Use of colloid filtration theory in modeling movement of bacteria through a contaminated sandy aquifer, *Environ. Sci. Technol.*, 25, 178–185, 1991.
- Johnson, P. R., and M. Elimelech, Dynamics of colloid deposition in porous media: Blocking based on random sequential adsorption, *Langmuir*, 11, 801–812, 1995.
- Johnson, P. R., N. Sun, and M. Elimelech, Colloid transport in geochemically heterogeneous porous media: Modeling and measurements, *Environ. Sci. Technol.*, 30, 3284–3293, 1996.
- Johnson, W. P., K. A. Blue, B. E. Logan, and R. G. Arnold, Modeling bacterial detachment during transport through porous media as a residence-time-dependent process, *Water Resour. Res.*, 31(11), 2649–2658, 1995.
- Kallay, N., and E. Matijevic, Diffusional detachment of colloidal particles from solid/liquid solution interfaces, *Adv. Colloid Interface Sci.*, 27, 1–42, 1987.
- Kokotovich, P., Method of sensitivity points in the investigation and optimization of linear control systems, *Autom. Remote Control*, 25, 1512–1518, 1964.
- Kreindler, E., On the definition and application of the sensitivity function, *J. Franklin Inst.*, 285(1), 26–36, 1968.
- Kretzschmar, R., M. Borkovec, D. Grolimund, and M. Elimelech, Mobile subsurface colloids and their role in contaminant transport, *Adv. Agron.*, 66, 121–193, 1999.
- Kuiper, L., A comparison of several methods for the solution of the inverse problem in two-dimensional steady state groundwater flow modeling, *Water Resour. Res.*, 22(5), 705–714, 1986.
- McCarthy, J. F., and C. Degueldre, Sampling and characterization of colloids and particles in groundwater for studying their role in contaminant transport, in *Environmental Particles, Environmental Analytical and Physical Chemistry Series*, edited by J. Buffle and H. P. van Leeuwen, A. F. Lewis, New York, 1993.
- McCaulou, D. R., R. C. Bales, and J. F. McCarthy, Use of short-pulse experiments to study bacteria transport through porous media, *J. Contam. Hydrol.*, 15, 1–14, 1994.
- McDowell-Boyer, L. M., Chemical mobilization of micron-sized particles in saturated porous media under steady flow conditions, *Environ. Sci. Technol.*, 26, 586–593, 1992.
- McLaughlin, D., and L. R. Townley, A reassessment of the groundwater inverse problem, *Water Resour. Res.*, 32(5), 1131–1161, 1996.
- Meinders, J. M., J. Noordmans, and H. J. Busscher, Simultaneous monitoring of the adsorption and desorption of colloidal particles during deposition in a parallel plate flow chamber, *J. Colloid Interface Sci.*, 152, 265–280, 1992.
- Mishra, S., and S. C. Parker, Parameter estimation for coupled unsaturated flow and transport, *Water Resour. Res.*, 25(3), 670–682, 1989.
- Penrod, S. L., T. M. Olson, and S. B. Grant, Deposition kinetics of two viruses in packed beds for quartz granular media, *Langmuir*, 12, 5576–5587, 1996.
- Pieper, A. P., J. N. Ryan, R. W. Harvey, G. L. Amy, T. H. Illangsekare, and D. W. Metge, Transport and recovery of bacteriophage PRD1 in a sand and gravel aquifer: Effect of sewage-derived organic matter, *Environ. Sci. Technol.*, 31, 1163–1170, 1997.
- Roy, S. B., and D. A. Dzombak, Colloid release and transport processes in natural and model porous media, *Colloid Surf. A*, 107, 245–262, 1996.
- Rubin, Y., and S. Ezzedine, The travel times of solutes at the Cape Cod tracer experiment: Data analysis, modeling, and structural parameters inference, *Water Resour. Res.*, 33(7), 1537–1547, 1997.
- Ruckenstein, E., and D. C. Prieve, Adsorption and desorption of particles and their chromatographic separation, *AIChE J.*, 22, 276–283, 1976.

- Ryan, J. N., and M. Elimelech, Colloid mobilization and transport in groundwater, *Colloid Surf. A*, 107, 1–52, 1996.
- Ryan, J. N., and P. M. Gschwend, Effects of ionic strength and flow rate on colloid release: Relating kinetics to intersurface potential energy, *J. Colloid Interface Sci.*, 164, 21–34, 1994.
- Ryan, J. N., M. Elimelech, R. A. Ard, and R. W. Harvey, Bacteriophage PRD1 and silica colloid transport and recovery in an iron oxide-coated sand aquifer, *Environ. Sci. Technol.*, 33, 63–73, 1999.
- Saiers, J. E., G. M. Hornberger, and L. Liang, First- and second-order kinetics approaches for modeling the transport of colloidal particle in porous media, *Water Resour. Res.*, 30(9), 2499–2506, 1994a.
- Saiers, J. E., G. M. Hornberger, and C. Harvey, Colloidal silica transport through structured, heterogeneous porous media, *J. Hydrol.*, 163, 271–288, 1994b.
- Scholl, M. A., and R. W. Harvey, Laboratory investigation on the role of sediment surface and groundwater chemistry in transport of bacteria through a contaminated sandy aquifer, *Environ. Sci. Technol.*, 26, 1410–1417, 1992.
- Scholl, M. A., A. L. Mills, J. S. Herman, and G. M. Hornberger, The influence of mineralogy and solution chemistry on the attachment of bacteria to representative aquifer materials, *J. Contam. Hydrol.*, 6, 321–336, 1990.
- Sim, Y., and C. V. Chrysikopoulos, Analytical models for one-dimensional virus transport in saturated porous media, *Water Resour. Res.*, 31(5), 1429–1437, 1995.
- Sim, Y., and C. V. Chrysikopoulos, Three-dimensional analytical models for virus transport in saturated porous media, *Transp. Porous Media*, 30(1), 87–112, 1998.
- Song, L., P. R. Johnson, and M. Elimelech, Kinetics of colloid deposition onto heterogeneously charged surfaces in porous media, *Environ. Sci. Technol.*, 28, 1164–1171, 1994.
- Sun, N., Colloid transport in physically and geochemically heterogeneous porous media: Modeling, measurements, and parameter identification, Ph.D. dissertation, Univ. of Calif., Los Angeles, 1998.
- Sun, N.-Z., *Mathematical Modeling of Groundwater Pollution*, Springer-Verlag, New York, 1995.
- Sun, N.-Z., *Inverse Problems in Groundwater Modeling*, Kluwer Acad., Norwell, Mass., 1994.
- Sun, N.-Z., and W. W.-G. Yeh, Coupled inverse problem in groundwater modeling, 1, Sensitivity analysis and parameter identification, *Water Resour. Res.*, 26(10), 2507–2525, 1990.
- Tien, C., *Granular Filtration of Aerosols and Hydrosols*, Butterworth-Heinemann, Woburn, Mass., 1989.
- Tomovic, R., *Sensitivity Analysis of Dynamic Systems*, translated from Russian by D. Tornquist, McGraw-Hill, New York, 1963.
- Valocchi, A. J., Validity of the local equilibrium assumption for modeling sorbing solute transport through homogeneous soils, *Water Resour. Res.*, 21(6), 808–820, 1985.
- Yan, Y. D., Pulse-injection chromatographic determination of the deposition and release rate constants of colloidal particles in porous media, *Langmuir*, 12, 3383–3388, 1996.
- Yeh, W. W.-G., Review of parameter identification procedures in groundwater hydrology: The inverse problem, *Water Resour. Res.*, 22(2), 95–108, 1986.

M. Elimelech and N. Sun, Environmental Engineering Program, Department of Chemical Engineering, Yale University, P.O. Box 208286, New Haven, CT 06520-8286. (menachem.elimelech@yale.edu; ning.sun@yale.edu)

J. N. Ryan, Department of Civil, Environmental, and Architectural Engineering, University of Colorado, Boulder, CO 80203. (Joseph.Ryan@colorado.edu)

N.-Z. Sun, Department of Civil and Environmental Engineering, University of California, Los Angeles, Los Angeles, CA 90095. (nezheng@seas.ucla.edu)

(Received March 14, 2000; revised September 11, 2000; accepted September 18, 2000.)